Earth and Planetary Science Letters 357-358 (2012) 130–136

Contents lists available at SciVerse ScienceDirect

Earth and Planetary Science Letters

journal homepage: www.elsevier.com/locate/epsl

Radiative heat transfer in a hydrous mantle transition zone

Sylvia-Monique Thomas [a,*], Craig R. Bina [a], Steven D. Jacobsen [a], Alexander F. Goncharov [b]

[a] Department of Earth and Planetary Sciences, Northwestern University, Evanston, IL 60208, USA
[b] Geophysical Laboratory, Carnegie Institution of Washington, Washington, DC 20015, USA

ARTICLE INFO

Article history:
Received 16 February 2012
Received in revised form
5 August 2012
Accepted 20 September 2012
Editor: L. Stixrude

Keywords:
Optical absorption spectroscopy
ringwoodite
wadsleyite
thermal conductivity
Earth's mantle
Earth's transition zone

ABSTRACT

The structure and dynamics of Earth's interior depend crucially upon heat flow and thus upon the thermal conductivity of its constituents. We measured optical absorbance spectra of hydrous wadsleyite and hydrous ringwoodite at simultaneous high-pressure and high-temperature conditions up to 26 GPa and 823 K in order to determine their radiative conductivities and to study the potential influence of hydration in the transition zone on thermal conductivity of the mantle. We report radiative thermal conductivities of $1.5 \pm 0.2\ Wm^{-1}K^{-1}$ for hydrous wadsleyite and $1.2 \pm 0.1\ Wm^{-1}K^{-1}$ for hydrous ringwoodite at transition zone conditions. The analytically derived radiative thermal conductivities of anhydrous wadsleyite and ringwoodite are 40% and 33% higher, respectively. The total thermal conductivities, calculated from temperature- and pressure-dependent optical absorption measurements, maintain an energy transmission window in the infrared and visible spectral range at high pressures and temperatures. The results indicate that the mantle transition zone may contribute significantly to heat transfer in the mantle and demonstrate the importance of radiative heat transfer in controlling geodynamic processes in Earth's mantle.

1. Introduction

Heat in Earth's interior is transported by convection and conduction. Temperature- and pressure-dependent thermal conductivity of mantle materials is an important parameter for geodynamic models of mantle convection (e.g., Dubuffet et al., 2000, 2002; Matyska et al., 1994; van den Berg et al., 2001). The bulk thermal conductivity has two components: lattice conductivity (k_{lat}) and radiative conductivity (k_{rad}) (e.g., Clark, 1957; Schatz and Simmons, 1972). Whereas lattice conductivity is governed by phonon propagation, radiative conductivity arises from heat transport by emission and absorption of photons (e.g., Hofmeister, 2005, 2010). The latter, therefore, can be indirectly measured by analyzing the visible and infrared (vis–IR) regions of a material's optical absorption spectrum because absorption bands provide a mechanism for diffusive radiative transfer (Hofmeister, 2004). Thermal conductivity in the mantle is controlled by temperature, pressure, the electronic structure and concentration of transition metal ions (such as iron), and the water content of the material (Clark, 1957; Hofmeister, 2004).

Until recently, radiative heat transfer was considered relatively unimportant in the mantle. Earlier experimental work suggested that most ferromagnesian mantle minerals become opaque in the vis–IR range at high-pressure due to intensification and red-shift of Fe^{2+}–Fe^{3+} charge-transfer bands (Mao, 1976; Mao and Bell, 1972). More recent studies show some mantle minerals such as ringwoodite remain transparent at high pressure (Keppler and Smyth, 2005), and thus radiative conductivity could contribute to the total heat flux of the Earth's mantle (Dubuffet et al., 2000, 2002). The total thermal conductivity, including k_{lat} and k_{rad}, and its dependence upon temperature, pressure, and composition, is essential for accurate models of heat flow in Earth (Dubuffet et al., 2000, 2002; Hofmeister, 2004). For example, Hofmeister (2004) showed that structurally incorporated $(OH)^-$ in nominally anhydrous minerals can contribute significantly to their total thermal conductivity by providing a mechanism for radiative diffusion of heat. At 1500 K, Hofmeister (2004) reports for sub-cm-sized olivine with ~10–100 wt ppm H_2O a magnitude of k_{rad} of ~1/8 of the lattice contribution to k_{tot} of olivine. The presence of H_2O enhances diffusion rates, promotes the growth of large grains, allows steeper temperature gradients, affects flow and fabric and can be invoked to explain slab behaviour (Hofmeister, 2004; Jung and Karato, 2001). Models suggest that a larger k_{rad} may stabilize planforms of mantle convection (Dubuffet et al., 2000, 2002) and allow greater heat loss and faster cooling of material. Other theoretical work shows that without the addition of radiative conductivities to geodynamic models of Earth's lower mantle, geophysical inferences of mega-plumes are difficult to explain (Matyska et al., 1994; van den Berg et al., 2001). However, experimental results on temperature effects upon radiative heat transfer were not available, and absolute

* Corresponding author. Present address: Department of Geoscience, University of Nevada Las Vegas, Las Vegas, NV 89154, USA.
E-mail address: sylvia-monique.thomas@unlv.edu (S.-M. Thomas).

0012-821X/$ - see front matter © 2012 Elsevier B.V. All rights reserved.
http://dx.doi.org/10.1016/j.epsl.2012.09.035

k_{rad} values were uncertain. Instead, olivine spectra were used to model mantle heat transfer and it was assumed that denser phases have similar spectral features (e.g., Hofmeister, 2005).

Most previous work focused on Earth's upper and lower mantle and assumed grain sizes of 0.1–1 cm (e.g., Fukao et al., 1968; Goncharov et al., 2006, 2010; Keppler et al., 2008; Shankland et al., 1979). Experimentally derived thermal conductivity values for the lower mantle are inconclusive and vary by an order of magnitude (Goncharov et al., 2006; Hofmeister, 2010; Keppler et al., 2008). Recent experiments suggest a lower mantle thermal conductivity of 8–9 $Wm^{-1}K^{-1}$ (Manthilake et al., 2011). Little is known about the mantle transition zone at 410–660 km depth, which constitutes about 7.5% of Earth's mass. The transition zone is thought to consist mainly of high-pressure polymorphs of olivine, wadsleyite and ringwoodite, along with garnet–majorite solid solutions (Ringwood, 1991). The thermal conductivity of the transition zone contributes to the regulation of heat flux between lower and upper mantle. The transition zone may be critical to the dynamics of the entire mantle because many subducted slabs appear to stagnate there, and because the transition zone minerals wadsleyite and ringwoodite have the highest H_2O storage capacity among mantle minerals.

Previous measurements of thermal conductivity in mantle minerals include work at high pressures and room temperature (Goncharov et al., 2006, 2010; Keppler et al., 2008; Keppler and Smyth, 2005), at high temperature and room pressure (Shankland et al., 1979), and at simultaneous *P–T* conditions, to 20 GPa and 1373 K (Xu et al., 2004). Manthilake et al. (2011) measured k_{lat} of Al-and Fe-bearing silicate perovskite up to 26 GPa and 1073 K, and ferropericlase with a range of Fe-contents up to 14 GPa and 1273 K. These studies have led to implications for radiative heat transfer and estimates of the lattice thermal conductivity of mantle material. However, there is a lack of data about the radiative conductivity of transition zone minerals, especially under hydrous conditions and at simultaneous high pressures and temperatures. Earlier studies on radiative thermal conductivity in wadsleyite and majorite (Keppler and McCammon, 1996; Ross, 1997) concluded that those minerals are relatively unimportant for heat transfer. Other studies (Keppler and Smyth, 2005) showed that ringwoodite might contribute to radiative heat transfer in the mantle, but the effect of temperature at high pressure has not been determined. Theoretical models have estimated temperature-pressure variation of thermal conductivity (e.g., Stackhouse and Stixrude, 2010), without, however, accounting for radiative contributions. Future models can benefit from experiments at conditions relevant to Earth's mantle. Here, we studied the effect of pressure, temperature and hydration on the optical absorption spectrum of wadsleyite and ringwoodite at mantle conditions.

2. Material and methods

2.1. Sample syntheses and characterisation

Gem-quality single crystals of Fo_{90}-composition hydrous wadsleyite and hydrous ringwoodite were synthesized at 18 GPa and 1400 °C in the 5000-ton multi-anvil apparatus at the Bayerisches Geoinstitut, Bayreuth, Germany by Smyth et al. (2003) (ringwoodite, run SZ0104) and by Jacobsen (wadsleyite, run Z570, see Mao et al., 2011). The ringwoodite crystals from run SZ0104 are reported to contain 1.07 wt% H_2O by FTIR (Smyth et al., 2003), in good agreement with 1.11 wt% H_2O measured by secondary ion mass spectrometry (SIMS) (Mao et al., 2011) and 0.9 wt% H_2O measured by Raman spectroscopy using the technique from Thomas et al. (2009). The average ferric iron content of the hydrous ringwoodite is about 10% (Smyth et al., 2003). Hydrous Fo_{90}-wadsleyite crystals came from run Z570 and contain 1.9(2) wt% H_2O as determined by SIMS (Mao et al., 2011), which is in fairly good agreement with a value of 1.4 wt% H_2O determined by FTIR using the absorption coefficient established in Deon et al. (2010). Mössbauer spectroscopy shows the wadsleyite also contains about 10% ferric iron (Mao et al., 2011).

2.2. Optical absorption spectroscopy

For optical absorption measurements in the IR–vis–UV spectral range (400–50000 cm^{-1}), 50 to 60 μm-sized optically clear single-crystals of ringwoodite (blue) and wadsleyite (green) were doubly polished to thicknesses of 13 μm, and 18 and 19 μm, respectively. Samples were loaded in resistively heated diamond-anvil cells with type IIa diamonds (300 μm culet size) and argon as the pressure medium (Figs. S1–S3). Several ruby spheres were placed next to the sample, and pressure was determined using the pressure-dependent energy shift of the R_1 ruby fluorescence line (Mao et al., 1986; Goncharov et al., 2005). Additional experimental details can be found in the supplementary material.

UV–vis spectra were acquired using the 300 grooves/mm grating of an Acton Research Corporation Spectra Pro 500-i spectrometer with a 0.5 m triple grating monochromator and a system of all-reflecting relay optics with double confocal geometry. A combined deuterium/halogen lamp served as the light source, focused to ~20 μm diameter at the sample. Unpolarised IR-spectra were obtained with a Varian Resolution Pro 670-IR spectrometer. For each spectrum, 1024 scans were accumulated in the range of 400–10000 cm^{-1}, using a quartz (2800–10000 cm^{-1}) or KBr (400–6000 cm^{-1}) beam splitter with 4 cm^{-1} resolution. After taking measurements at high pressure and room temperature (Figs. S4 and S5), ringwoodite was studied at 26 GPa up to 650 °C, and wadsleyite spectra were recorded at 15 GPa up to 450 °C. At each pressure and temperature, spectra through the sample and the reference spectrum through diamonds and pressure medium were obtained for the flat-field correction.

For data analysis the spectra from three (UV–vis–IR) spectral ranges were merged after correction for reflection losses and sample thickness to produce the final spectrum. The typical photon path length estimated from optical absorption spectra is on the order of ~200 μm. This allows a proper description of the radiative part of heat conduction in the deep Earth, as it is smaller than the grain size in the Earth's mantle 0.1–1 cm (Keppler et al., 2008). Spectra were fitted using Peakfit software of Jandel Scientific. A linear baseline subtraction was applied. The linear baseline subtraction was only used to characterize the absorption bands and determine band positions. The basis for thermal conductivity calculations used measured spectra corrected exclusively for thickness and reflection losses.

2.3. Correction for reflection losses in measured spectra

Corrections for reflection losses were carried out according to Keppler et al. (2008). The absorbance A_R due to reflection was subtracted from the measured absorbance. A_R was calculated from the reflectivity given by the Fresnel formula

$$A_R = -2\log(1-R)$$

$$R = (n_{sample}-n_{Ar})^2/(n_{sample}+n_{Ar})^2$$

where n_{sample} and n_{Ar} are the refractive indices of sample and argon, respectively. For argon a pressure-dependent refractive index was utilised (Grimsditch et al., 1986). We used a constant refractive index of 1.76 for wadsleyite and 1.77 for ringwoodite (Anthony et al., 1995). The net result of this approximation on the measured absorption spectra is negligible (<0.007 absorbance units). Moreover, the correction for reflection losses affects the results very moderately (<0.007 absorbance units), which is within the experimental

uncertainty related to non-reproducibilities in sample positioning and probing beam vignetting. The refractive indices of wadsleyite and ringwoodite are expected to increase with pressure, but no experimental data are available that would allow a more precise calculation, so we assumed pressure-independent refractive indices. A 30% pressure-induced refractive index change for wadsleyite and ringwoodite would result in a reflection correction of <0.05 absorbance units, which is within the experimental uncertainty. Also, we multiplied measured absorption coefficients by ln 10 to obtain absorption coefficients based on the natural logarithm. Further discussion of experimental uncertainties can be found in the supplementary material.

2.4. Infrared spectroscopy

Unpolarised IR spectra of doubly polished platelets of wadsleyite and ringwoodite (Figs. S7 and S9) were recorded from 2000–4000 cm^{-1} with a Bruker Tensor 37 FTIR spectrometer equipped with a Hyperion 2000 IR microscope, a MCT detector, a KBr beamsplitter and a globar light source with a 50×50 μm aperture. Up to 512 scans were taken with a resolution of 2 cm^{-1}. The sample thickness was determined using the spacing between visible-wavelength interference fringes and confirmed by the eyepiece reticule and stage micrometre scale of the Hyperion 2000 microscope. A linear baseline subtraction was applied for the purpose of characterizing absorption bands. The basis for thermal conductivity calculations were as-measured spectra corrected exclusively for thickness and reflection losses. The sum of experimental uncertainties can contribute to up to ~10% error in calculated conductivity values (see supplementary material).

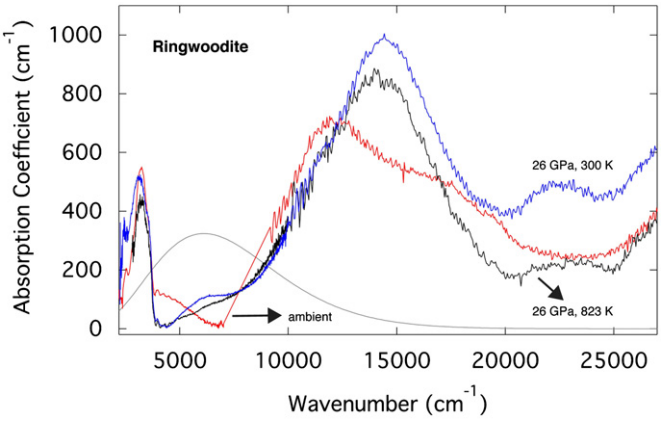

Fig. 1. Optical absorption spectra of Fe-bearing hydrous ringwoodite at room pressure, prior to compression (red), at 26 GPa and 300 K (blue), and at 26 GPa and 823 K (black). Initial sample thickness is 13 μm. The solid grey line represents the calculated blackbody radiation (arbitrary units) at 1800 K. (For interpretation of the references to colour in this figure legend, the reader is referred to the web version of this article.)

3. Results

3.1. Ambient conditions

At ambient pressure the UV–vis absorption spectrum of hydrous ringwoodite reveals a crystal field band at 11700 cm^{-1} ($^5T_{2g}$–^5E_g transitions of Fe^{2+} in the octahedral site), an intervalence charge transfer (IVCT) band (Fe^{2+} to Fe^{3+}) at 16300 cm^{-1}, and an absorption edge due to ligand–metal charge transfer (Keppler and Smyth, 2005) (O^{2-} to Fe^{2+}) close to 30000 cm^{-1} (Fig. 1, Table 1). The hydrous wadsleyite spectrum at ambient conditions is characterized by a similar absorption edge in the UV–vis range, two broad bands at 9800 cm^{-1} and 14200 cm^{-1} corresponding to the crystal field and intervalence charge transfer bands, respectively, and a weak band at 23100 cm^{-1} (Fig. 3). Differences in crystal field (CF) band positions in the spectra of the two high-pressure polymorphs of olivine can be explained by different cation–oxygen distances in the octahedral site of ringwoodite (Smyth et al., 2003, Thomas et al., 2008) as compared to the octahedral site in wadsleyite (Deon et al., 2010, Mao et al., 2011). In ringwoodite the octahedral site has a strong centrosymmetric character with high regularity (e.g., Taran et al., 2009). The large widths of the CF bands (Table 1) are likely due to superposition of overlapping CF bands arising from Fe^{2+} in different octahedral sites, M1, M2, and M3, which have very similar characteristics (e.g., Ross, 1997). The positions of the IVCT bands are comparable to what has been observed previously in minerals with edge-shared octahedra (Burns, 1993; Ross, 1997; Keppler and Smyth, 2005). The large widths of the IVCT bands are characteristic features of such IVCT transitions in minerals (Mattson and Rossman, 1987), which also cause the intense colour of the specimens.

In the infrared part of the spectrum, both samples show bands caused by OH stretching vibrations (Figs. 1, 2, S7 and S9). The hydrous ringwoodite spectrum shows maxima at ~2500, 3106, 3341, 3556, and 3656 cm^{-1}. The feature at ~2500 cm^{-1} has been assigned to overtones by Mattson and Rossman (1987). The hydrous wadsleyite spectrum shows strong bands at 3336, 3384, 3588, 3612, and 3650 cm^{-1}. Details about OH band assignments can be found elsewhere (Hofmeister and Mao, 2001; Smyth et al., 2003; Jacobsen et al., 2005; Thomas et al., 2008; Deon et al., 2010).

3.2. Pressure dependence

With increasing pressure, CF and IVCT bands shift to higher frequencies in both materials (Table 1), similar to what has been observed for ringwoodite (Keppler and Smyth, 2005) and other minerals (Mattson and Rossman, 1987), but contrary to earlier presumptions for wadsleyite (Burns, 1993). In contrast, the UV-edge shows a 3000 cm^{-1} pressure-dependent red-shift with the low-energy tail covering part of the visible range, which is typical for Fe-bearing minerals (Mao, 1976, Taran et al., 2009). With increasing pressure, the width and linear absorption coefficient of the CF band in wadsleyite increase; the latter by a factor of 3 from 452 cm^{-1} to 1406 cm^{-1}, as opposed to the peak height and width of the IVCT band, which decrease by 47% and 26%, respectively (Table 1). In ringwoodite, the width and peak height of the CF band also increases but only by about 37% (compared with a factor of three for wadsleyite). Intensification of the CF band was not observed for ringwoodite by Keppler and Smyth (2005), but it has been observed before in other minerals (e.g., Mattson and Rossman, 1987). The increase in peak height of the CF band has been explained as intensification due to charge-fluctuation effects (Mattson and Rossman, 1987) of Fe^{2+} with Fe^{3+}, which occupy neighbouring structurally equivalent positions in edge-sharing octahedra (Akimoto et al., 1976). For ringwoodite the peak height and width of the IVCT band decrease by ~74% and 62%, respectively. The fact that CF and IVCT bands show different pressure dependences supports the assignment of those bands to different centres. The decrease of the IVCT band has been explained before as pressure-induced reduction of Fe^{3+} in the ringwoodite structure (Taran et al., 2009), which is thought to be a reversible process. In a previous study (Taran et al., 2009) the IVCT band completely disappeared at a low pressure of ~9 GPa, which is contrary to our observations of the IVCT band remaining visible at the maximum experimental pressure.

Table 1
Band assignment and characterisation for wadsleyite and ringwoodite.

Band assignment (cm^{-1})	Position (cm^{-1})	Peak height = linear absorption coefficient (cm^{-1})	Width (cm^{-1})	Width-shift (cm^{-1}/GPa)/(cm^{-1}/K)	Band-shift (cm^{-1}/GPa)	Band-shift (cm^{-1}/K)
Wadsleyite (this study)						
Fe^{2+}: $^5T_{2g}$–^5E_g	9800 ± 100	452	2975	54/1.12	81	−1.12
Fe^{2+}-Fe^{3+} intervalence charge transfer	14200 ± 100	483	4905	−41/1.82	117	−1.00
Fe^{3+}: $^6A_{1g}$–$^4A_{1g}$	23100 ± 200	31	2033	–	–	–
Ringwoodite (this study)						
Fe^{2+}: $^5T_{2g}$–^5E_g	11700 ± 100	525	4332	23/0.7	104	−0.32
Fe^{2+}-Fe^{3+} intervalence charge transfer	16300 ± 200	365	6183	−147/0.13	231	−0.46
Ringwoodite (Keppler and Smyth, 2005)						
Fe^{2+}: $^5T_{2g}$–^5E_g	8678	71	2291	–	–	–
Fe^{2+}: $^5T_{2g}$–^5E_g	12265	320	5012	–	78	–
Fe^{2+}–Fe^{3+} intervalence charge transfer	17482	183	5798	–	146	–
Wadsleyite (Ross, 1997)						
Fe^{2+}: $^5T_{2g}$–^5E_g	8902	82	3315	–	–	–
Fe^{2+}: $^5T_{2g}$–^5E_g	11136	105	2736	–	–	–
Fe^{2+}–Fe^{3+} intervalence charge transfer	13374	76	3520	–	–	–
Fe^{2+}–Fe^{3+} intervalence charge transfer	15921	46	3607	–	–	–

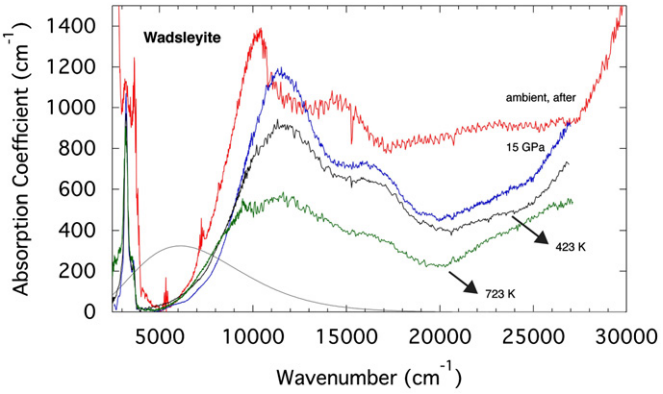

Fig. 2. Optical absorption spectra of Fe-bearing hydrous wadsleyite at 15 GPa and 300 K (blue), at 15 GPa and 423 K (black), and at 15 GPa and 723 K (green) and after decompression at room pressure and temperature (red). Initial sample thickness is 18 μm. The solid grey line represents the calculated blackbody radiation (arbitrary units) at 1800 K. (For interpretation of the references to colour in this figure legend, the reader is referred to the web version of this article.)

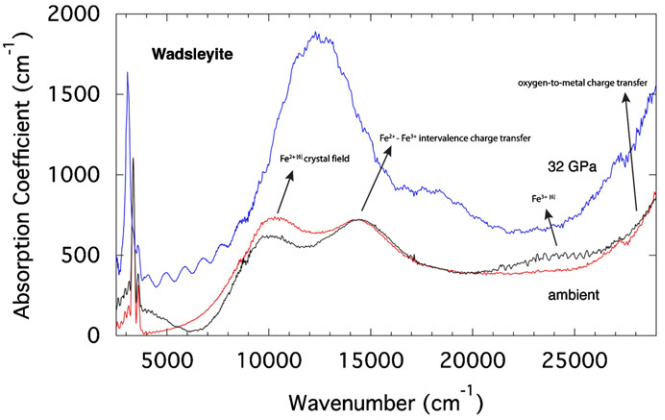

Fig. 3. Optical absorption spectra of Fe-bearing hydrous wadsleyite at room pressure, prior to compression (red), at the highest pressure of 32 GPa (blue), and after decompression back to room pressure (black). Initial sample thickness is 19 μm. (For interpretation of the references to colour in this figure legend, the reader is referred to the web version of this article.)

3.3. Temperature dependence

With increasing temperature, the CF and IVCT bands shift to lower frequencies, linear absorption coefficients of the bands decrease, and bandwidths increase, all in a continuous manner (Table 1). Also on increasing temperature, the CF and IVCT bands do not intensify and band broadening is not sufficient to close the transparency window in the sample spectra. Similar behaviour of Fe^{2+}/Fe^{3+} IVCT bands has been previously observed for ringwoodite (Taran et al., 2009), involving a relatively weak temperature-dependent intensity decrease of the CF band and stronger temperature dependence for the IVCT band. However, CF and IVCT bands in ringwoodite studied here at high pressure and high temperature show similar but stronger temperature dependences, whereas the CF band in wadsleyite has a stronger temperature response than the IVCT band.

The absorption spectra (Figs. 1–3) show significant changes at high pressure and high temperature. Optical photomicrographs (Figs. S1–S3) illustrate the transparent nature of the samples throughout the experiment. The results indicate that at transition zone conditions, where the maximum of energy flux at 1800 K is around ~6200 cm^{-1} (Figs. 2 and 3), the effect of pressure and temperature on the absorption spectra of transition zone minerals enables energy transmission in the near-infrared region (Figs. 1 and 2).

3.4. Radiative thermal conductivity

From the optical absorption spectra, we calculated the radiative thermal conductivity using analytically corrected spectra and the formalism of Fukao et al. (1968). We followed the traditional approach (Clark, 1957; Fukao et al., 1968) in order to allow for meaningful comparison with the majority of the existing measurements and calculations (Schatz and Simmons, 1972; Mao, 1976; Jung and Karato, 2001; Xu et al., 2004; Keppler and Smyth, 2005; Goncharov et al., 2006; Keppler et al., 2008; Taran et al., 2009; Stackhouse and Stixrude, 2010). However, we note that all such calculations may be subject to additional corrections for fractional emissivity and grain size (e.g., Shankland et al., 1979; Hofmeister, 2004, 2005; Hofmeister and Yuen, 2007). We used 1800 K as reference temperature for the transition zone and calculated the radiative thermal conductivity from all spectra.

Based on our 300 K spectra, the values of radiative conductivity for hydrous ringwoodite and hydrous wadsleyite in the transition zone are 1.0 $Wm^{-1}K^{-1}$ (26 GPa) and 1.9 $Wm^{-1}K^{-1}$ (15 GPa), respectively (Fig. 4). At transition zone pressures and temperatures,

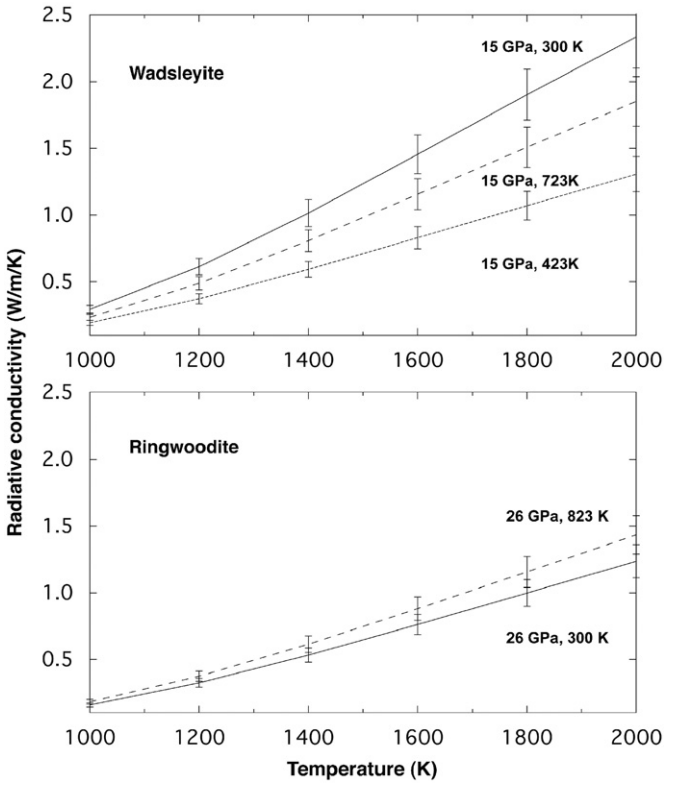

Fig. 4. Calculated radiative conductivity of hydrous wadsleyite and hydrous ringwoodite as a function of temperature. Calculations are based on the 15 GPa/300 K, 15 GPa/423 K and 15 GPa/723 K spectra shown in Fig. 2 for wadsleyite, and on the ambient, 26 GPa/300 K and 26 GPa/823 K spectra shown in Fig. 1 for ringwoodite. Error bars represent a 10% uncertainty of the radiative conductivity values.

the value increases to 1.2 $Wm^{-1} K^{-1}$ for hydrous ringwoodite but decreases to 1.5 $Wm^{-1} K^{-1}$ for hydrous wadsleyite (Fig. 4). The observed differences between ringwoodite and wadsleyite support the idea that ferromagnesian minerals may exhibit different radiative conductivities and pressure- and temperature-dependent behaviour. Our results also imply that room P-T absorption spectra should not be used to infer radiative conductivities at high pressures and temperatures and further show that olivine should not be used as a model mineral for the denser polymorphs.

4. Discussion

4.1. Implications for heat transfer in a hydrated transition zone

We present radiative thermal conductivities determined from simultaneous high-pressure and high-temperature optical absorption measurements of hydrous wadsleyite and ringwoodite. Thermal conductivity in the transition zone affects Earth's heat flow, thermal evolution, and mode of mantle convection. Our values for hydrous wadsleyite and ringwoodite are comparable to the values determined for anhydrous olivine (Shankland et al., 1979) with k_{rad} of $\sim$2 $Wm^{-1} K^{-1}$ for $(Mg_{0.9},Fe_{0.1})SiO_4$ at 1700 K. Shankland et al. (1979) observed only a weak temperature dependence of absorption above 800 K and further observed upon increasing temperature a rise in band intensity, band broadening, and a small positive wavenumber shift. Ringwoodite should have a higher lattice thermal conductivity than wadsleyite, and wadsleyite is expected to have $\sim$30% higher k_{lat} than olivine (Xu et al., 2004). Taking into account the conductivities determined from high-temperature/high-pressure spectra, we observe the opposite relationship for the radiative conductivity, where wadsleyite has a k_{rad} $\sim$25% higher than ringwoodite.

According to Hofmeister (1999), the radiative contribution to heat flow in the transition zone is very small, with k_{rad} $\sim$0.49 $Wm^{-1} K^{-1}$ at 660 km depth, about 10–15% of the total thermal conductivity. The lattice contribution on the other hand dominates, yielding k_{tot} of 4.7 $Wm^{-1} K^{-1}$. However, Hofmeister (1999) noted potential uncertainties resulting from actual mantle temperatures and the amount of ringwoodite taken into consideration, which due to its high k_{tot} dominates the value of the bulk conductivity. For Mg–ringwoodite, Hofmeister (1999) presented an ambient k_{tot} value of 7.7 $Wm^{-1} K^{-1}$. Hofmeister (1999) also suggests that for Fe-contents of $\sim$10%, k_{tot} would be reduced by $\sim$0.5 $Wm^{-1} K^{-1}$ to a value of 7.2 $Wm^{-1} K^{-1}$, similar to our results for ringwoodite. Using equation 12 from Xu et al. (2004) and the reported measured ambient thermal conductivities allows us to calculate the lattice part of the thermal conductivity for wadsleyite and ringwoodite at 1800 K and at 15 and 26 GPa, respectively. For wadsleyite, k_{lat} is 4.4 $Wm^{-1} K^{-1}$, while k_{lat} for ringwoodite is 5.9 $Wm^{-1} K^{-1}$. Adding our calculated k_{rad} values results in a k_{tot} for wadsleyite of 5.9 $Wm^{-1} K^{-1}$ and for ringwoodite 7.1 $Wm^{-1} K^{-1}$. Thus, the total thermal conductivity of ringwoodite is $\sim$21% higher than the value for wadsleyite, representing a similar, only somewhat larger increase than expected (Xu et al., 2004). Our ringwoodite k_{tot} value is in very good agreement with the 7.2 $Wm^{-1} K^{-1}$, calculated by Hofmeister (1999) for Fe-bearing ringwoodite and $\sim$1.1 $Wm^{-1} K^{-1}$ larger than the conductivity determined by Xu et al. (2004), which might be due to their assumption that k_{rad} is negligible. The radiative conductivities calculated herein (20–30% of k_{tot}) are larger than those anticipated by Hofmeister (1999), who estimated k_{rad} to be about 10–15% of the total conductivity.

4.2. Effect of hydration on radiative heat transfer

In the previous discussion we assumed a hydrous transition zone. Subtracting the OH stretching bands between 2200 cm^{-1} and 4000 cm^{-1} in the infrared region of the spectra, extrapolating a linear baseline (thus assuming higher transparency) and calculating radiative thermal conductivity results in a 40% higher k_{rad} value for ringwoodite of 1.6 $Wm^{-1} K^{-1}$, and a 33% higher k_{rad} value for wadsleyite of 2.1 $Wm^{-1} K^{-1}$ (Fig. 5). In contrast to the hydrous TZ model, k_{rad} values are $\sim$2 $Wm^{-1} K^{-1}$ for both polymorphs, which is in good agreement with the reported k_{rad} value of $\sim$2 $Wm^{-1} K^{-1}$ for anhydrous olivine at 1700 K (Shankland et al., 1979). Our results imply that a water content of $\sim$1 wt% H_2O lowers the thermal radiative conductivity of ringwoodite and wadsleyite by 40 or 33%, respectively (Fig. 5). According to equation 12 from Xu et al. (2004) and the extrapolated ambient thermal conductivities to 1800 K and 15 and 26 GPa, a dry transition zone would have a total k_{tot} of 6.5 $Wm^{-1} K^{-1}$ for wadsleyite and 7.5 $Wm^{-1} K^{-1}$ for ringwoodite. Hydration significantly affects thermal conductivity in the upper mantle as discussed previously by Hofmeister (2004), who also derived a formula for $k_{rad,\ wet}$ that is independent of structure and chemical composition. Grain-size dependent k_{rad} values for olivine have been calculated for a temperature of 1500 K (Hofmeister, 2004). All of those values for a range of grain sizes from 0.01 to 10 cm are magnitudes smaller (0.008–0.04 $Wm^{-1} K^{-1}$) than our values for ringwoodite and wadsleyite with a water content of $\sim$1 wt%. We stress that either high water contents or large grain sizes limit radiative heat transfer. However, assuming the effect of grain size on k_{rad} to be rather small for minerals with very high water contents (cf. Fig. 5 in Hofmeister, 2004), our k_{rad} values imply that hydration effects in the transition zone would be higher than expected.

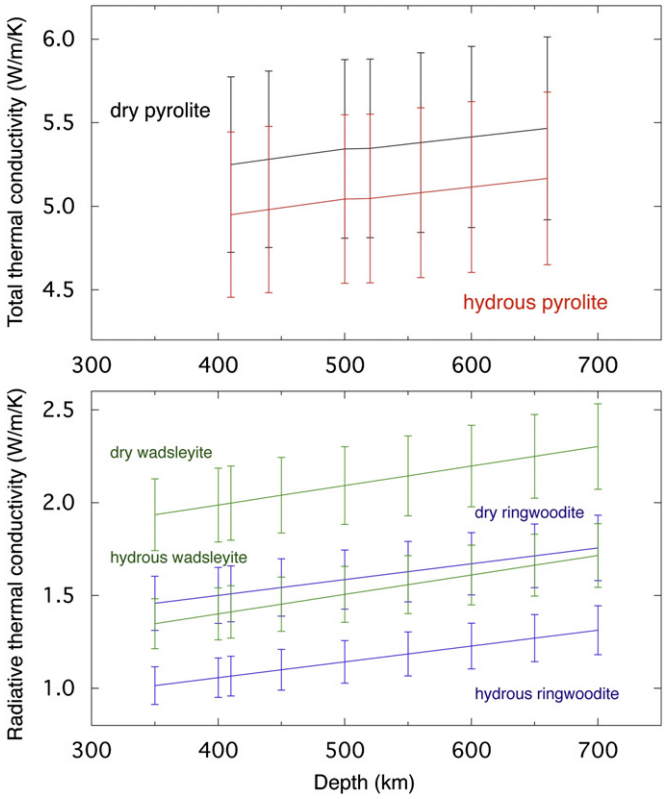

Fig. 5. The total thermal conductivity across the mantle transition zone (~ 410–660 km) was calculated using data from this study and the geotherm from Ito and Katsura (1989). The mantle transition zone is modelled as pyrolitic mixture of 60% wadsleyite and ringwoodite, and 40% majorite. Majorite thermal conductivity values are based on data from Giesting et al. (2004) and equation 12 from Xu et al. (2004). Error bars represent a 10% uncertainty of the radiative conductivity values.

5. Conclusions

Our results imply that the radiative conductivities of transition zone minerals may have been underestimated thus far. Our calculated k_{rad} values represent ~22–32% of k_{tot} for a dry transition zone model and ~17–26% of k_{tot} for a hydrous transition zone, which are twice previous estimates (Hofmeister, 2004). Our estimates that k_{rad} is ~20–30% of k_{tot} represent a maximum contribution of radiative conductivity because they were obtained from measurements on single-crystal samples. Effective values could be lower because of internal and grain boundary scattering effects and due to stronger IR absorbance in garnet (e.g. Shankland et al., 1979).

This study shows from experiments that pressure and temperature conditions in the mantle exert a strong effect on the radiative conductivities of ringwoodite and wadsleyite. Values calculated from high-pressure, high-temperature spectra differ significantly from values determined at ambient conditions. The phonon contribution of thermal conductivity decreases with temperature, making heat conduction by radiation more important. Differences in radiative thermal conductivities of transition zone mineral assemblages will affect models of lithospheric geotherms, subduction dynamics, and the structure of lithospheric slabs (Hofmeister, 1999; Marton et al., 2005; Maierová et al., 2012). However, the extent to which radiative thermal conductivity affects geothermal models requires further evaluation. The presence of a strong radiative component would enable increased heat flow with temperature, thereby stabilizing large plume structures (Keppler et al., 2008; van den Berg et al., 2001). Lower k_{rad} values on the other hand enhance the extent to which much of Earth's internal heat is removed by convection and decreases the ability of thermal models involving conduction and radiation alone to explain thermal conditions in the mantle (Shankland et al., 1979). Further quantification of the influence of radiative thermal conductivity will require refined thermal models of Earth's dynamic interior.

Acknowledgements

This research was supported by the NSF EAR-0748707 (S.D.J.) and EAR-1015239 (A.F.G.), DOE/BES, DOE/NNSA (CDAC), and by the David and Lucile Packard Foundation. We thank N. Blair for access to the FTIR microscope at Northwestern University, D.J. Frost for help with synthesis of wadsleyite sample Z570, J.R. Smyth for ringwoodite samples from run SZ0104, and D. McInerney for help with the thermal conductivity model. We also acknowledge Y. Fukao, and H. Keppler for discussions.

Appendix A. Supporting information

Supplementary data associated with this article can be found in the online version at http://dx.doi.org/10.1016/j.epsl.2012.09.035.

References

Akimoto, et al., 1976. High-pressure crystal chemistry of orthosilicates and the formation of the mantle transition zone. In: Strens, R.G.J. (Ed.), The Physics and Chemistry of Minerals and Rocks, John Wiley, London, pp. 327–363.
Anthony, et al., 1995. Handbook of Mineralogy, Vol. 2, Silica, Silicates. Mineral Data Publishing, pp. 904.
Burns, R.G., 1993. Mineralogical Applications of Crystal Field Theory, 2nd ed. Cambridge University Press, Cambridge, UK, pp. 551.
Clark, S.P., 1957. Absorption spectra of some silicates in the visible and near infrared. Am. Miner. 42, 732–742.
Deon, et al., 2010. Location and quantification of hydroxyl in wadsleyite: new insights. Am. Miner. 95, 312–322.
Dubuffet, et al., 2000. Feedback effects of variable thermal conductivity on the cold downwellings in high Rayleigh number convection. Geophys. Res. Lett. 27 (18), 2981–2984.
Dubuffet, et al., 2002. Controlling thermal chaos in the mantle by positive feedback from radiative thermal conductivity. Nonlinear Processes Geophys. 9, 311–323.
Fukao, et al., 1968. Optical absorption spectra at high temperatures and radiative thermal conductivity of olivines. Phys. Earth Planet. Inter. 1, 57–62.
Giesting, et al., 2004. Thermal conductivity and thermodynamics of majoritic garnets: implications for the transition zone. Earth Planet. Sci. Lett. 218, 45–56.
Goncharov, et al., 2005. Optical calibration of pressure sensors for high pressures and temperatures. J. Appl. Phys. 97 094917-1–5.
Goncharov, et al., 2006. Reduced radiative conductivity of low-spin (Mg, Fe)O in the lower mantle. Science 312, 1205–1208.
Goncharov, et al., 2010. Effect of composition, structure, and spin state on the thermal conductivity of the Earth's lower mantle. Phys. Earth Planet. Inter. 180, 148–153.
Grimsditch, et al., 1986. Refractive index determination in diamond anvil cells: results for argon. J. Appl. Phys. 60, 3479–3481.
Hofmeister, A.M., 1999. Mantle values of thermal conductivity and the geotherm from phonon lifetimes. Science 283, 1699–1706.
Hofmeister, A.M., 2004. Enhancement of radiative transfer in the upper mantle by OH^- in minerals. Phys. Earth Planet. Inter. 146, 483–495.
Hofmeister, A.M., 2005. Dependence of diffusive radiative transfer on grain-size, temperature, and Fe-content: implications for mantle processes. J. Geodyn. 40, 51–72.
Hofmeister, A.M., 2010. Scale aspects of heat transport in the diamond anvil cell, in spectroscopic modeling, and in Earth's mantle: implications for secular cooling. Phys. Earth Planet. Inter. 180, 138–147.
Hofmeister, A.M., Mao, H.K., 2001. Evaluation of shear moduli and other properties of silicates with the spinel structure from IR spectroscopy. Am. Miner. 86, 622–639.
Hofmeister, A.M., Yuen, D.A., 2007. Critical phenomena in thermal conductivity: implications for lower mantle dynamics. J. Geodyn. 44, 186–199.
Ito, E., Katsura, T., 1989. A temperature profile of the mantle transition zone. Geophys. Res. Lett. 16, 425–428.

Jacobsen, et al., 2005. A systematic study of OH in hydrous wadsleyite from polarized FTIR spectroscopy and single-crystal X-ray diffraction: oxygen sites for hydrogen storage in Earth's interior. Am. Miner. 90, 61–70.
Jung, H., Karato, S.I., 2001. Water-induced fabric transitions in olivine. Science 293, 1460–1463.
Keppler, H., McCammon, C.A., 1996. Crystal field and charge transfer spectrum of (Mg, Fe)SiO_3 majorite. Phys. Chem. Miner. 23, 94–98.
Keppler, H., Smyth, J.R., 2005. Optical and near infrared spectra of ringwoodite to 21.5 GPa: implications for radiative heat transport in the mantle. Am. Miner. 90, 1209–1212.
Keppler, et al., 2008. Optical absorption and radiative thermal conductivity of silicate perovskite to 125 Gigapascals. Science 322, 1529–1532.
Maierová, et al., 2012. The effect of variable thermal diffusivity on kinematic models of subduction. J. Geophys. Res. 117, B07202 (14 pp).
Manthilake, et al., 2011. Lattice thermal conductivity of lower mantle minerals and heat flux from Earth's core. Proc. Natl. Acad. Sci. USA 108, 17901–17904.
Mao, H.K., 1976. Charge transfer process at high pressure. In: Strens, R.G.J. (Ed.), The Physics and Chemistry of Minerals and Rocks. Wiley, London, pp. 573–581.
Mao, H.K., Bell, P.M., 1972. Electrical conductivity and the red shift of absorption in olivine and spinel at high pressure. Science 176, 403–405.
Mao, et al., 1986. Calibration of the ruby pressure gauge to 800 kbar under quasi-hydrostatic conditions. J. Geophys. Res. 91, 4673–4676.
Mao, et al., 2011. Effect of hydration on the single-crystal elasticity of Fe-bearing wadsleyite to 12 GPa. Am. Miner. 96, 1606–1612.
Marton, et al., 2005. Effect of variable thermal conductivity on the mineralogy of subducting slabs and implications for mechanisms of deep earthquakes. Phys. Earth Planet. Inter. 149, 53–64.
Mattson, S.M., Rossman, G.R., 1987. Identifying characteristics of charge transfer transitions in minerals. Phys. Chem. Miner. 14, 94–99.
Matyska, et al., 1994. The potential influence of radiative heat transfer on the formation of megaplumes in the lower mantle. Earth Planet. Sci. Lett. 125, 255–266.
Ringwood, A.E., 1991. Phase transformations and their bearing on the constitution and dynamics of the mantle. Geochim. Cosmochim. Acta 55, 2083–2110.
Ross, N., 1997. Optical absorption spectra of transition zone minerals and implications for radiative heat transport. Phys. Chem. Earth 22, 113–118.
Schatz, J.F., Simmons, G., 1972. Thermal conductivity of Earth materials at high temperatures. J. Geophys. Res. 77, 6966–6983.
Shankland, et al., 1979. Optical absorption and radiative heat transport in olivine at high temperature. J. Geophys. Res. 84, 1603–1610.
Smyth, et al., 2003. Structural systematics of hydrous ringwoodite and water in the Earth's interior. Am. Miner. 88, 1402–1407.
Stackhouse, S., Stixrude, L., 2010. Theoretical methods for calculating the lattice thermal conductivity of minerals. In: Wentzcovitch, R., Stixrude, L. (Eds.), Theoretical and Computational Methods in Mineral Physics: Geophysical Applications: Reviews in Mineralogy and Geochemistry, 71; 2010, pp. 253–269.
Taran, et al., 2009. Spectroscopic studies of synthetic and natural ringwoodite, γ-$(Mg,Fe)_2SiO_4$. Phys. Chem. Miner. 36, 217–232.
Thomas, et al., 2008. Protonation in germanium equivalents of ringwoodite, anhydrous phase B and superhydrous phase B. Am. Miner. 93, 1282–1294.
Thomas, et al., 2009. IR calibrations for water determination in olivine, r-GeO_2 and SiO_2 polymorphs. Phys. Chem. Miner. 36, 489–509.
van den Berg, et al., 2001. The effects of variable thermal conductivity on mantle heat-transfer. Geophys. Res. Lett. 28, 875–878.
Xu, et al., 2004. Thermal diffusivity and conductivity of olivine, wadsleyite and ringwoodite to 20 GPa and 1373 K. Phys. Earth Planet. Inter. 143–144, 321–336.